



# Ozone decrease observed in the upper atmosphere following the May 11<sup>th</sup> 2024 *Mother's day* solar storm.

Alexandre Winant<sup>1,2</sup>, Viviane Pierrard<sup>1,2</sup>, and Edith Botek<sup>1</sup>

<sup>1</sup>Solar Wind, Space Physics and Solar-Terrestrial Center of Excellence, Royal Belgian Institute for Space Aeronomy (BIRA-IASB), Avenue Circulaire 3, Brussels, Belgium

<sup>2</sup>Center for Space Radiations (CSR), Earth and Life Institute, Climate Sciences ELI-C, Université Catholique de Louvain (UCLouvain), Louvain-la-Neuve, Belgium

**Correspondence:** Alexandre Winant (alexandre.winant@aeronomie.be)

**Abstract.** On May 11<sup>th</sup> 2024, a succession of coronal mass ejections that merged together struck the Earth and induced large scale perturbations in the magnetosphere. During this event, satellite observations showed a large solar energetic proton (SEP) event associated to an extreme geomagnetic storm. At the same time, satellite observations of atmospheric ozone have been performed by AURA/MLS. In this work, we present the first observations of the effect of the storm of May and the following SEP of June 8<sup>th</sup> on ozone concentration throughout the atmosphere. Observations of the MLS show that the event of May lead to stronger depletion of  $O_3$  in the upper part of the atmosphere than in June. This difference is explained by the type of particle precipitation that occurred during the two events, with both protons and electrons in May and only protons in June. Neither event caused ozone depletion in the stratosphere while strong decreases are observed in the mesosphere. In May, mesospheric ozone depletion is observed during 18 days and reaches a maximum of 60%. In addition, the storm of May also caused a noticeable decrease in ozone concentration (up to 20%) at altitudes above 90 km.

## 1 Introduction

While solar cycle 25 is approaching its maximum activity (predicted in 2025), the probability of strong solar events is also expected to rise. Both the frequency and the intensity of solar events increase around the maximum and the declining phase of the cycle. The year 2024 is located at the end of the ascending phase of cycle 25, making it prone to be subjected to large perturbations of solar origin. On the 11<sup>th</sup> of May 2024, an extreme geomagnetic storm associated with a large Forbush decrease in galactic cosmic rays were observed on the ground Mavromichalaki et al. (2024). The cause of the extreme event of May 2024 is a succession of CMEs (Coronal Mass Ejections) that merged together and simultaneously struck the Earth, which lead to an extreme perturbation of the magnetosphere Kwak et al. (2024). Moreover, a large Solar Energetic Particle (SEP) event was observed in the vicinity of the Earth by space borne particle detectors Pierrard et al. (2024). This geomagnetic storm is the largest observed in more than 20 years, reaching a minimum Disturbed Storm time index  $Dst_{min} = -412$  nT and a maximum Bartels planetary index of geomagnetic activity  $Kp_{max} = 9$ . The last observation of an event with a similar magnitude dates back to the famous 2003 Halloween geomagnetic storm with a minimum  $Dst_{min}$  around  $-400$  nT. The geomagnetic storm of May 11<sup>th</sup> was responsible for large variations in the radiation belts of the Earth, in which a temporary 4



belts structure was observed at low Earth orbit Pierrard et al. (2024). On the 8<sup>th</sup> of June 2024, 27 days after the extreme event  
25 of May, another SEP event has been observed near Earth.

Enhanced geomagnetic activity also leads to increased energetic electron precipitation (EEP) in the atmosphere at high  
latitude which mainly consist of auroral electrons originating from the magnetotail and radiation belt electrons in the bounce  
loss cone. Energetic protons of solar origin also precipitate in the atmosphere as they are guided toward high latitudes by  
the Earth's magnetic field. As they penetrate into the atmosphere, energetic particles interact with the constituents of the  
30 atmosphere inducing their excitation, dissociation and ionization Sinnhuber et al. (2012); Mironova et al. (2015). Following  
the interaction of the atmosphere with the energetic precipitating particles (EPP), complex chains of chemical reactions take  
place in different layers of the atmosphere which can lead to the formation of odd hydrogen ( $HO_x = H + HO + HO_2$ ) and odd  
nitrogen ( $NO_x = N + NO + NO_2$ ) via ion-neutral chemistry Verronen and Lehmann (2013).  $NO_x$  are mainly produced in the  
upper part of the atmosphere, in the mesosphere (50 to 90 km) and lower thermosphere, where their production rate is increased  
35 by EPP Sætre et al. (2004). Those species are long lived in the atmosphere, especially during polar winter. In the presence of the  
polar vortex,  $NO_x$  produced in the mesosphere and lower thermosphere (MLT) region can be efficiently transported downward  
to the stratosphere (10 to 50 km in average) and deplete the ozone in this region of the atmosphere Randall et al. (2007); Funke  
et al. (2014, 2016). Mesospheric  $HO_x$  levels have been observed to correlate with the precipitation of electrons from the  
radiation belts Verronen et al. (2011); Andersson et al. (2012).  $HO_x$  are short lived, thus their response to EPP is localized in  
40 space and time, where and when ionization is increased Mironova et al. (2015).  $HO_x$  and  $NO_x$  contribute to the depletion of  
ozone through catalytic reactions Lary (1997). Thus, the net result of EPP is to contribute to decrease the ozone concentration  
in the atmosphere and can have repercussion on climate Rozanov et al. (2012); Seppälä et al. (2014).

The response of ozone in the atmosphere to EPP (of both protons and electrons) has been extensively studied over the years.  
Energetic Electron Precipitations (EEP) have been found to have a significant influence on  $O_3$  in the mesosphere between 60 km  
45 and 80 km, where it could be depleted by 90% on a short term scale Andersson et al. (2012). Because they have the possibility  
to ionize lower layers in the atmosphere, energetic solar protons may contribute to deplete ozone in the upper stratosphere.  
However, strong evidence of SEP directly depleting stratospheric ozone are scarce. In the study of Jia et al. (2020), changes of  
ozone were observed by MLS after SEPs between 2004 up to 2020. Although clear ozone depletion can be observed at high  
altitudes following multiple SEPs, only one event was found to have an effect on the stratospheric ozone.

50 In this paper, we use observations from the Microwave Limb Sounder (MLS) to investigate and provide a first report of the  
effect of the extreme solar and geomagnetic event of May as well as the following SEP of June on atmospheric ozone in the  
polar regions.

## 2 Data and methods

### 2.1 Ozone observations from AURA/MLS

55 The Microwave Limb Sounder (MLS) as part of the Earth Observing System (EOS) Evans and Greer (2000) was launched in  
2004 onboard the NASA satellite AURA on quasi-polar sun-synchronous orbit at 705 km of altitude. This instrument measures



thermal radiation from Earth's atmosphere retrieving vertical profiles of the temperature and trace gases by scanning Earth's limb in the plane of its orbit. In this work, we mainly use ozone profiles from the MLS that are derived from radiances measured by the 240 GHz radiometer. More specifically, we use the latest version v5.0 of the MLS data product with a spatial coverage ranging from  $-82^\circ$  to  $82^\circ$  and that has an increased vertical range compared to previous versions. With v5.0, ozone observations in the upper mesosphere are available for scientific studies. In this work, we have applied all recommendations regarding data screening provided in the *MLS Level 2 Version 5 Quality Document* that can be found at ([https://mls.jpl.nasa.gov/data/v5-0\\_data\\_quality\\_document.pdf](https://mls.jpl.nasa.gov/data/v5-0_data_quality_document.pdf)). Moreover, we only use high latitude observations, comprised between  $60^\circ$  and  $90^\circ$  in both hemispheres and then perform daily averages which are necessary for the highest altitudes in the mesosphere. (Level 2 ozone data from MLS are available at [https://disc.gsfc.nasa.gov/datasets/ML2O3\\_005/summary](https://disc.gsfc.nasa.gov/datasets/ML2O3_005/summary), last accessed on 29/10/2024)

## 2.2 In situ observations of energetic particles

For the solar proton fluxes, we use the observations from the Geostationary Operational Environmental Satellite (GOES) which is fitted with the Energetic Proton, Electron, and Alpha Detector (EPEAD). This instrument measures the flux of protons in 7 energy channels spanning from 0.74 to 900 MeV. The data used in this work consists of integral proton fluxes with energies  $> 10$  MeV,  $> 30$  MeV,  $> 100$  MeV which have a resolution of 5 minutes. (Data are accessible at: <https://lasp.colorado.edu/space-weather-portal/>, last accessed on 29/10/2024)

In order to determine when energetic electrons from the radiation belts precipitate into the atmosphere, we use the POES/MEPED detector. The MEPED instrument is composed of two pairs of directional detectors. The first pair is dedicated to the measurement of protons with energies ranging from 30 keV to 200 MeV. The second pair of detectors measures the fluxes of electrons of energies between 30 keV to 2500 keV in 3 integral channels. For a given type of particles, the two telescopes are arranged perpendicular to one another and are referred to as the  $0^\circ$  telescope and the  $90^\circ$  telescope. On MetOp, the  $0^\circ$  telescope points directly to the zenith and the  $90^\circ$  telescope points to the antiram direction (i.e., opposite to the velocity vector of the spacecraft). At high latitudes, the  $0^\circ$  telescope mainly measures particles in the Bounce Loss Cone (BLC) and thus precipitating into the atmosphere.

## 2.3 Assessing the impact on ozone and temperature

The main strategy to quantify the effect of the May and June events on ozone through the atmosphere is taking the average profile of ozone before the event (quiet ozone profile), and computing its difference relative to the daily profiles for the rest of the month. The quiet period consists of the five daily profiles observed before either the maximum proton flux observed by GOES or the minimum in the Dst index. Those profiles are then averaged on time to provide the quiet conditions.

Another approach used in this work is to first compute the long term trend in the profiles observed by MLS. In order to do so, a lowess (locally weighted scatter plot smoothing) algorithm was applied to the daily profiles from MLS spanning from January 1<sup>st</sup> 2024 to June 30<sup>th</sup>. With the results of the lowess algorithm, the daily detrended profiles are computed, revealing only the short term variations which can then be compared to daily averaged geomagnetic activity.



### 3 Results

90 Figure 1 shows the daily averaged MLS ozone profiles at high latitudes from the beginning of 2024 to June 30<sup>th</sup>. The top panel corresponds to the high southern latitudes comprised between -60° and -90° of latitude and the middle panel corresponds to the northern latitudes comprised between 60° and 90°. The last panel of this figure shows the geomagnetic activity for the period, displaying both the Dst and Kp indices. The bottom panel of the figure indicates that during the beginning of the year, the geomagnetic activity is very low, with the Kp index barely exceeding 4. It is only in March that a noticeable geomagnetic  
95 storm was recorded in both Dst and Kp. The next big event took place in mid April with a Dst below -100 nT and a Kp of 7. From this point onward, these indices show that the magnetosphere was repeatedly disrupted by intense storms until the extreme event of May 11 occurred with a minimum Dst value never seen in 20 years of -412 nT and a Kp of 9. During the recovery phase of this major event, some other intense events took place and the Dst index remained quiet until the end of June.

All along this period, the AURA/MLS instrument continuously carried out measurements of ozone throughout the atmo-  
100 sphere. The first panel of Fig. 1 clearly illustrates the different ozone layers that exist in the atmosphere. The main ozone layer located in the stratosphere, the secondary layer in the upper mesosphere and lower thermosphere (MLT) region and finally the tertiary layer in the mesosphere where the maximum of ozone concentration is observed at around 75 km. Both the second and third ozone layers are subjected to very strong seasonal variations and are mostly depleted during local summer due to increased photodissociation Marsh et al. (2001); Smith and Marsh (2005); Smith et al. (2018).

105 Thus in the northern hemisphere (NH), the ozone forming the secondary and tertiary layers gradually gets depleted from winter to summer, when the mesospheric ozone is completely removed from the atmosphere and the secondary layer ozone is reduced from between 7 and 8 ppmv to between 1 and 2 ppmv. In the southern hemisphere (SH) (middle panel of Fig. 1), the situation is reversed and ozone starts to accumulate in the mesosphere and the lower thermosphere.

In addition to the strong seasonal variations of ozone, the first and second panel of the figure clearly show that the ozone  
110 also experiences short term variations. Those variations on smaller time scales are not linked to geomagnetic storms illustrated by high peaks of geomagnetic activity in the bottom panel, in any of the ozone layers.

In order to observe a direct effect of solar energetic particles (SEP) in the stratospheric ozone layer, there must be a significant flux of protons with sufficient energy to ionize the stratosphere. Between January and May, some minor SEP events did occur but they had low fluxes and a soft spectrum which could not have impacted the stratospheric ozone. Soft protons can deposit  
115 their energy in the mesosphere, and some rapid decreases in  $O_3$  happened in the NH after the particles injections at high altitudes, but not always. After the May 11 events, no ozone is left in the upper part of the atmosphere so that no ozone is lost further. Despite their hard spectrum and high fluxes, neither the May nor the June SEPs (see Fig. 2) have had any impact on the NH main ozone layer. One of the reasons might be due to the weakening of the polar vortex in the NH during late spring and summer.

120 In the SH, in the beginning of the year, no short term variation of  $O_3$  has been observed by MLS. However, the middle panel of Fig. 1 clearly shows a change of ozone concentration in the MLT region (at  $\sim 90$  km) as well as in the mesosphere (at  $\sim 75$  km) after the event of May. In the stratosphere, no sign of the event of May is discernible in the figure.

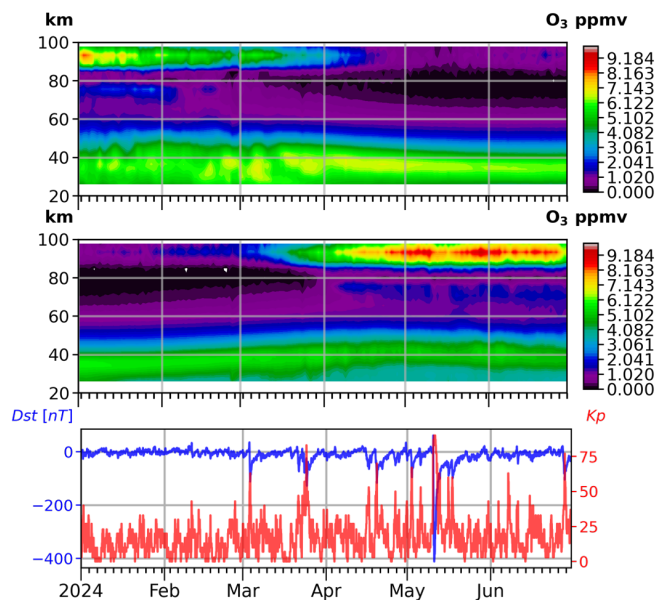


**Figure 1.** Daily averaged high latitude ( $[60^\circ, 90^\circ]$ ) ozone volume mixing ratio profiles from AURA/MLS as a function of time and altitude between January 1<sup>st</sup> and June 30<sup>th</sup> 2024. Top: northern hemisphere. Middle: southern hemisphere. Ozone volume mixing ration is expressed in parts per million by volume (ppmv). Bottom: Geomagnetic activity indices from the OMNI database between January 1<sup>st</sup> and June 30<sup>th</sup>. The Disturbed storm time (Dst) index is represented in blue and the planetary Kp index multiplied by 10 is displayed in red.

The flux of EPP between May 1<sup>st</sup> and June 30<sup>th</sup> 2024 are presented on the two panels of Fig. 2. On the top, GOES observations of the integral proton fluxes with different energy threshold clearly show the two SEP events of May 11<sup>th</sup> and June 8<sup>th</sup>. This panel reveals that each of the two SEPs have a double peak in protons of  $> 10$  MeV and  $> 30$  MeV but not for protons with energies  $> 100$  MeV. The proton flux measured by GOES in June is very similar to the flux of May (see Fig. 2 top panel), because they originate from the same region of the Sun and they are separated in time by one solar rotation.

The second panel of Fig. 2 displays the integral flux of electrons with energies  $> 30$  keV observed by the MEPED  $0^\circ$  telescope during the same period as GOES. In this case, the electron fluxes are presented as a function L, the McIlwain parameter (uniquely identifying Earth's magnetic shells) and time. Electron fluxes have been averaged on L-time bins of 0.1 L and 3 hours. At high latitudes and thus high L values, electrons observed by the  $0^\circ$  telescope are considered to precipitate into the atmosphere along the magnetic field lines Rodger et al. (2010). Unlike SEP events, electron precipitation in the atmosphere is a process that is constantly occurring but it is modulated by geomagnetic activity. Increased precipitation has been observed during the main phase of the geomagnetic storm of May 11 reaching the maximum flux of  $\sim 1.2 \cdot 10^6$   $[\text{cm}^2 \text{s sr}]^{-1}$  which is never attained again throughout the whole period.

As ozone concentration in the atmosphere is subject to seasonal variations and changes on longer time scales such as the solar cycle, we computed the long term variations in the MLS observation in order to extract only the ozone changes on small

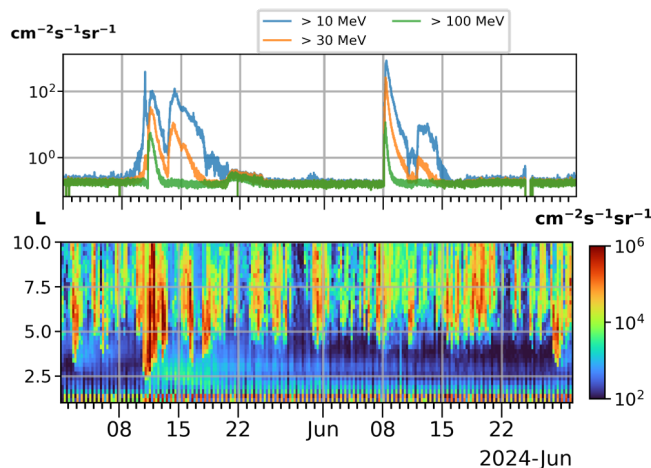


**Figure 2.** Top: Integral proton flux measured by GOES between May 01 and June 30, 2024 in three different energy channels. Bottom: Integral electron flux with energy  $>30$  keV measured by POES  $0^\circ$  telescope and averaged in L-time bins [0.1L - 3h] displayed as a function of time and the McIlwain parameter over the the same time period.

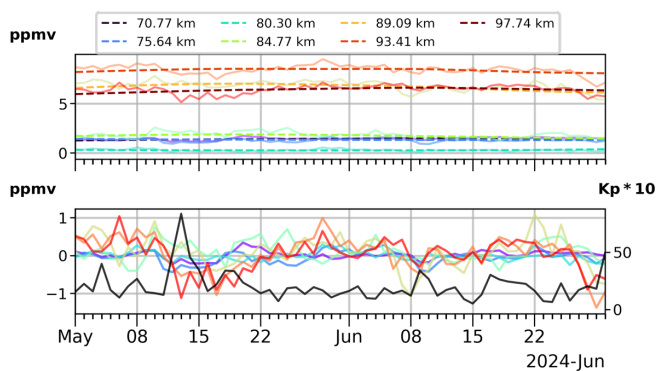


**Figure 3.** Top panel: The plain lines represent the daily averaged ozone vmr computed with AURA/MLS observations from May 1<sup>st</sup> and June 30<sup>th</sup> in the Southern hemisphere. The dashed lines are the computed long term trends in ozone vmr resulting from the lowess algorithm applied on the observations from January to June. Each color corresponds to an altitude level. Bottom panel: The daily detrended ozone vmr. Colors are the same as for the top panel. The black line represents the daily averaged Kp index multiplied by 10 computed from omni data.

time scales between May 1<sup>st</sup> and June 30<sup>th</sup>. The long term trend in MLS observations was computed by applying the lowess algorithm on the daily ozone profiles. To ensure that the results of the algorithm could capture the seasonal variability, we used the data from January 1<sup>st</sup> to June 30<sup>th</sup> to compute the trend. The result of this data treatment is shown in the top panel of Fig. 3 together with the daily average ozone volume mixing ratio (vmr). Each color in the figure represents an altitude level ranging from 70 km to 97 km, covering the mesosphere and lower thermosphere. The bottom panel of the figure shows the detrended



ozone vmr (i.e., daily ozone vmr minus the long term trend) at each altitude level. The black curve in this panel corresponds to the daily averaged Kp index (multiplied by 10) computed from the OMNI dataset. From this panel, it is clear that, following the peak in the Kp index which indicates the main phase of the geomagnetic storm of May 11<sup>th</sup>, a rapid decrease in ozone vmr is observed by the MLS. It then required 18 days for the ozone vmr to regain the pre-storm levels. In June, no major geomagnetic storm took place as shown by the daily Kp curve. However, the detrended ozone shows a noticeable decrease on the 7<sup>th</sup> of June at 84 km. At higher altitudes, the decrease in ozone occurs on the 9<sup>th</sup>, after the SEP event took place.

Figure 4 displays the results of the relative difference in percentage between the pre-storm (i.e. quiet) ozone vmr (top panel), as well as temperature profile (bottom panel) and all the daily profiles measured from the start of the period until the end of the month. The quiet period consists of the time averages of the daily profiles between May 5<sup>th</sup> and May 9<sup>th</sup>. The reason for not taking the profiles between the 6<sup>th</sup> and 10<sup>th</sup> is that, even if the peak of the SEP flux and the main phase of the geomagnetic storm took place on May 11<sup>th</sup>, the flux of lower energy protons (> 10 MeV) has a first peak on the 10<sup>th</sup> of May. So that May 10<sup>th</sup> is neither considered as a quiet day nor is the peak of the event (when considering the proton spectrum and the geomagnetic activity). The top panel shows the relative difference computed with  $O_3$  vmr and the bottom panel with temperature.

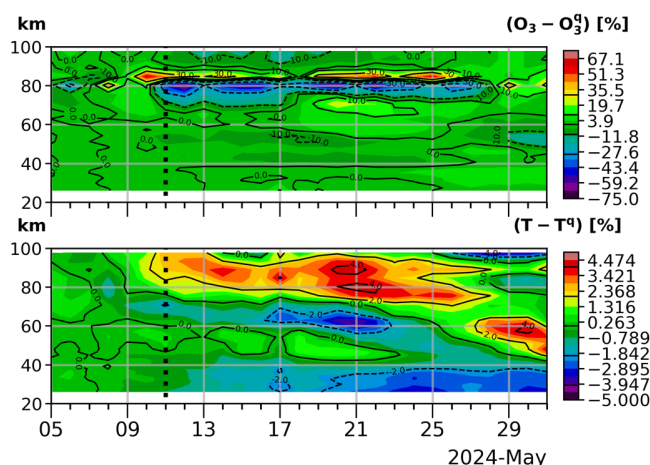


**Figure 4.** Top panel: Relative difference in [%] between the mean quiet condition ozone profiles ( $O_3^q$ ) and the daily ozone profiles from AURA/MLS, during the whole period between May 05 and May 30 ( $O_3$ ). Bottom: same for temperature profiles. Quiet conditions correspond to the period spanning from May 5 to May 9, 2024. The vertical black line displays the day when the daily Dst index reached its minimal value, indicating the end of the main phase of the geomagnetic storm on May 11 also corresponding to the peak proton flux for the event.

From the top panel of the figure, it is obvious that some ozone was lost during the period of interest. The vertical black dotted line indicates the day during which the daily averaged proton flux and geomagnetic activity are the highest (i.e. May 11<sup>th</sup>). The main ozone loss was observed after the event in the tertiary layer at around 75 km. However, the day before, on May 10<sup>th</sup>, the ozone vmr at those altitudes had already decreased by 20%. This premature decrease might be caused by the penetration of the low energy protons measured by GOES on that day, which efficiently deposit their energy around 70 km



(see Fig. 1 of Satori et al. (2016)). Two days after the main phase of the storm, ozone vmr at 80 km decreased by as much as 60%. This ozone deficit relative to pre-storm level remained until May 29<sup>th</sup>, oscillating between 30 % to 50%. Moreover, after the event until May 17<sup>th</sup>, the loss in ozone was observed in the tertiary layer between 70 km and 80 km. At those altitudes however, only around 20% of the ozone is depleted from the mesosphere. This ozone decrease is only observed down to 70 km  
165 until May 18<sup>th</sup>. In addition to the mesospheric ozone loss, in the MLT region above 90 km, a smaller depletion is observed by MLS. As for the lower altitudes, the decrease of ozone vmr in the MLT seems to start one day before the peak of the storm. However, the ozone loss is relatively small, mainly remaining below 10%. Nonetheless, the ozone depletion reached 20% and 15% on May 13<sup>th</sup> and 17<sup>th</sup> respectively corresponding to periods of increased electron precipitation (see Fig. 2 bottom panel). Finally, no significant change in  $O_3$  vmr has been observed by MLS after the storm of May in the stratosphere.

170 The bottom panel of Fig. 4 is the same as the top panel but for the temperature measurements from MLS. The changes observed during this period are confined between -5% and 5% through the entire altitude range. However, it is apparent in the figure that after the storm and SEP of May 11<sup>th</sup>, the entire atmosphere above 75 km heats up while below this altitude, the general trend is a cooling, except from May 27<sup>th</sup> to the 31<sup>th</sup> between 45 km and 70 km. It is important to note that the warming of the upper atmosphere starts two days before the event. As for the ozone, this premature atmospheric warming coincides with  
175 the early arrival of low energy protons in the atmosphere, as well as an early increase of electron precipitation before the SEP took place. Below 40 km, the temperature constantly decreases from the event onward. However, this change in temperature is caused by the seasonal variability. The heating observed in the upper part of the atmosphere is most likely caused by particle heating and joule heating. A part of the energy of the EPP is lost as heat in the atmosphere and some of its energy is dissipated when they move in the effective electric field of the Earth Sinnhuber et al. (2012).

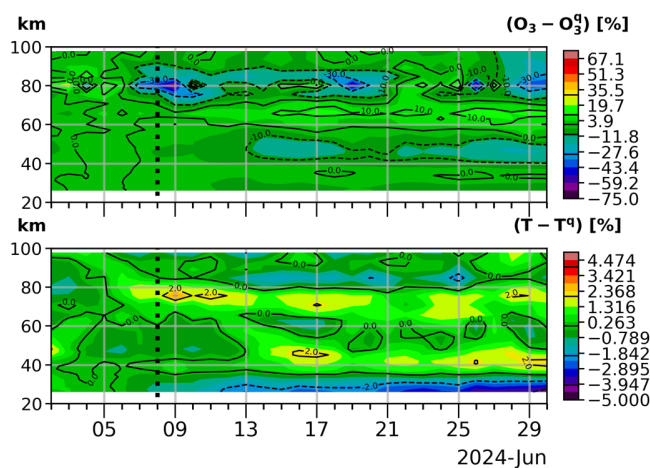


**Figure 5.** Top panel: Relative difference in [%] between the mean quiet condition ozone profiles ( $O_3^q$ ) and the daily ozone profiles from AURA/MLS, during the whole period between June 02 and June 30 ( $O_3$ ). Bottom: same for temperature profiles. Quiet conditions correspond to the period spanning from June 02 to June 07, 2024. The vertical black line displays the day of peak proton flux for this event.





180 The two panels of Fig. 5 are similar to those of Fig. 4 but for MLS observations just before and after the SEP of June  
8<sup>th</sup>. Again, the top panel shows the results for ozone. Despite being more intense than in May, this SEP had no influence  
on the stratospheric ozone. At around 50 km, the ozone vmr gradually decreases from the time of the SEP onward. Below  
this altitude, no noticeable change was observed by MLS. The slow ozone depletion at 50 km can be explained by long term  
(seasonal) variations rather than the effect of EPP (see Fig. 1 middle panel). The day following the proton injection of June,  
185 AURA/MLS measurements show a depletion of 60% in ozone vmr at 80 km. Although not as intense as at 80 km, the depletion  
in  $O_3$  vmr occurred between 70 km and 90 km and was of about 20%. In the MLT region, no change in ozone is discernible in  
the observations.

The bottom panel of the figure shows the relative difference in atmospheric temperature. The maximum changes in tem-  
perature observed in June are limited between -2% and 2%, which is quite less than in May. As in May, below 40 km, the  
190 temperature observations show a steady decrease caused by seasonal variations as winter starts in the SH. Between 40 km and  
80 km, the general behavior of the atmosphere is a small warming which is lasting for the whole period as is not likely to be  
linked to the proton precipitation.

#### 4 Discussion and conclusions

In this work, we presented the first observations of the atmospheric ozone response to the extreme geomagnetic storm and SEP  
195 that took place on May 11<sup>th</sup> and June 8<sup>th</sup> 2024. We mainly used AURA/MLS observations which provided measurements of  
ozone and temperature profiles at high latitude in both hemispheres due to its low Earth orbit.

The responses of ozone and temperature to the event of May 11<sup>th</sup> and June 8<sup>th</sup> are quite different. Much stronger and longer  
lasting ozone depletion is observed through the atmosphere in May than in June. However, this is easily explained by the  
difference in the flux of EPP during the two events. In May, an overlap between energetic solar protons observed by GOES  
200 and strongly enhanced electron fluxes from the radiation belts observed by POES have precipitated in the atmosphere. In June,  
electron precipitation is observed the day before the SEP reached the Earth, but does not continue due to the lack of strong  
geomagnetic disturbances for this event.

Aside the seasonal variations, there is a clear difference in the behavior of ozone in the northern and southern hemisphere  
after the precipitation of energetic particles in the high latitude atmosphere. During the event of May 11<sup>th</sup>, MLS observations  
205 show a clear decrease of ozone in the southern polar mesosphere. In the northern hemisphere however, only two short lived  
decreases in ozone took place in the MLT region above 90 km, on May 13<sup>th</sup> and on the 17<sup>th</sup>, each of them lasting for  
two days. These inter-hemispheric differences are strongly linked to the local season. For geomagnetic activity, hence electron  
precipitation, Mironova et al. (2023) showed through a one dimensional Radiative-Convective Photochemical model that ozone  
depletion in the mesosphere were only possible during local spring, winter and fall, with the strongest one only taking place in  
210 winter. Those conclusions also apply for solar protons as shown with MLS observations between 2004 and 2024 by Doronin  
et al. (2024) and by Xiong et al. (2023) for the severe SEP of January 2012. In our observations of the June SEP, no significant



changes in  $O_3$  were observed in the northern hemisphere whereas a drop of 60% occurred at 80 km in the polar southern hemisphere.

In the MLT region, decreases in ozone are only observed during the event of May 2024. At those altitudes, the maximum decrease in  $O_3$  is reached two days after the storm unlike in the mesosphere where it is reached in one day. In the MLT region, Jia et al. (2024) have discussed that the decrease in ozone are not linked to catalytic reactions with  $HO_x$  and  $NO_x$ , but rather to changes in the mean meridional circulation (MMC) induced by EPP. The perturbed MMC transports  $[O]$  and  $[H]$  in the polar MLT which, associated to the heating of the thermosphere, can lead to the decrease of ozone concentration. This process may explain the changes of ozone observed after the storm of May which featured a significant heating of the upper atmosphere. Furthermore, in June, no significant heating of the lower thermosphere was observed by MLS and no significant variation of ozone is observed. However, observations of  $[O]$  and  $[H]$  should be considered to verify this hypothesis.

Finally, measurements from MLS do not show a quick response of stratospheric ozone after the May and June events. In both cases, the spectrum of solar protons was hard enough to produce ionization in the upper stratosphere. In May, no significant change in ozone concentrations is observed below 60 km. This absence of response in stratospheric ozone could be explained by the season again. Indeed, Denton et al. (2018) have shown in the northern hemisphere with observations of 191 SEPs that ozone depletion following an event was never observed in absence of the polar vortex. Thus, stratospheric depletions are only visible during polar winter, which is not the case in May in the southern hemisphere. In June, ozone is depleted by 10% 5 days after the storm. However, this slow decrease in ozone over time is fitting the long term variation of ozone computed with the lowess algorithm. Moreover, even though June marks the winter in the SH, the decrease in ozone concentration observed by MLS is not consistent with a descent of  $NO_x$  from high altitudes, as no depletion is observed between 60 km and 70 km. In addition, a direct production of  $NO_x$  in the upper stratosphere would cause a decrease of ozone quickly after the storm, which is not observed here.

*Data availability.* All data are available in the zenodo Winant et al. (2024). OMNI data are available at <https://omniweb.gsfc.nasa.gov/ow.html>, Version 5 of MLS/Aura level 2 data and user recommendations can be found at <https://disc.gsfc.nasa.gov/datasets>, GOES proton integral fluxes can be found at [GOESdataareaccessibleat:https://lasp.colorado.edu/space-weather-portal/](https://lasp.colorado.edu/space-weather-portal/), MEPED electron fluxes are accessible at <https://lasp.colorado.edu/space-weather-portal/>

*Author contributions.* AW made the present analyses and wrote the manuscript with the contribution of the other authors. VP conceptualized and supervised the study, and contributed to the interpretation of the results. All authors contributed to writing of the manuscript through reviews and edits.

*Competing interests.* The author declare that they have no conflict of interests



*Acknowledgements.* The project 21GRD02 BIOSPHERE has received funding from the European Partnership on Metrology, co-financed by the European Union's Horizon Europe Research and Innovation Programme and by the Participating States. The authors acknowledge the Horizon 2020 PITHIA-NRF project with Grant Agreement 101007599.

245 The results presented in this document rely on data provided by the Community Coordinated Modeling Center at Goddard Space Flight Center through their integrated Space Weather Analysis (iSWA) system's HAPI server (<https://iswa.gsfc.nasa.gov/IswaSystemWebApp/hapi>). The CCMC is a multi-agency partnership between NASA, AFMC, AFOSR, AFRL, AFWA, NOAA, NSF and ONR. These data were accessed via the University of Colorado's Space Weather Technology, Research, and Education Center's (<https://colorado.edu/spaceweather>) Space Weather Data Portal (<https://lasp.colorado.edu/space-weather-portal>).



## References

- 250 Andersson, M. E., Verronen, P. T., Wang, S., Rodger, C. J., Clilverd, M. A., and Carson, B. R.: Precipitating radiation belt electrons and enhancements of mesospheric hydroxyl during 2004–2009, *Journal of Geophysical Research: Atmospheres*, 117, 2012.
- Denton, M. H., Kivi, R., Ulich, T., Clilverd, M. A., Rodger, C. J., and von der Gathen, P.: Northern hemisphere stratospheric ozone depletion caused by solar proton events: the role of the polar vortex, *Geophysical Research Letters*, 45, 2115–2124, 2018.
- Doronin, G., Mironova, I., Bobrov, N., and Rozanov, E.: Mesospheric Ozone Depletion during 2004–2024 as a Function of Solar Proton  
255 Events Intensity, *Atmosphere*, 15, 944, 2024.
- Evans, D. and Greer, M.: Polar orbiting environmental satellite space environment monitor, NOAA National Geophysical Data Center, 2000.
- Funke, B., López-Puertas, M., Stiller, G., and Von Clarmann, T.: Mesospheric and stratospheric NO<sub>y</sub> produced by energetic particle precipitation during 2002–2012, *Journal of Geophysical Research: Atmospheres*, 119, 4429–4446, 2014.
- Funke, B., López-Puertas, M., Stiller, G. P., Versick, S., and von Clarmann, T.: A semi-empirical model for mesospheric and stratospheric  
260 NO<sub>y</sub> produced by energetic particle precipitation, *Atmospheric Chemistry and Physics*, 16, 8667–8693, 2016.
- Jia, J., Kero, A., Kalakoski, N., Szeląg, M. E., and Verronen, P. T.: Is there a direct solar proton impact on lower-stratospheric ozone?, *Atmospheric Chemistry and Physics*, 20, 14969–14982, 2020.
- Jia, J., Murberg, L. E., Løvset, T., Orsolini, Y. J., Espy, P. J., Zeller, L. C., Salinas, C. C. J. H., Lee, J. N., Wu, D., and Zhang, J.: Energetic particle precipitation influences global secondary ozone distribution, *Communications Earth & Environment*, 5, 270, 2024.
- 265 Kwak, Y.-S., Kim, J.-H., Kim, S., Miyashita, Y., Yang, T., Park, S.-H., Lim, E.-K., Jung, J., Kam, H., Lee, J., et al.: Observational Overview of the May 2024 G5-Level Geomagnetic Storm: From Solar Eruptions to Terrestrial Consequences, *Journal of Astronomy and Space Sciences*, 41, 171–194, 2024.
- Lary, D.: Catalytic destruction of stratospheric ozone, *Journal of Geophysical Research: Atmospheres*, 102, 21515–21526, 1997.
- Marsh, D., Smith, A., Brasseur, G., Kaufmann, M., and Grossmann, K.: The existence of a tertiary ozone maximum in the high-latitude  
270 middle mesosphere, *Geophysical Research Letters*, 28, 4531–4534, 2001.
- Mavromichalaki, H., Papailiou, M.-C., Livada, M., Gerontidou, M., Paschalis, P., Stassinakis, A., Abunina, M., Shlyk, N., Abunin, A., Belov, A., et al.: Unusual Forbush Decreases and Geomagnetic Storms on 24 March, 2024 and 11 May, 2024, *Atmosphere*, 15, 1033, 2024.
- Mironova, I., Aplin, K. L., Arnold, F., Bazilevskaya, G. A., Harrison, R. G., Krivolutsky, A. A., Nicoll, K. A., Rozanov, E. V., Turunen, E., and Usoskin, I. G.: Energetic particle influence on the Earth’s atmosphere, *Space science reviews*, 194, 1–96, 2015.
- 275 Mironova, I., Grankin, D., and Rozanov, E.: Mesospheric ozone depletion depending on different levels of geomagnetic disturbances and seasons, *Atmosphere*, 14, 1205, 2023.
- Pierrard, V., Winant, A., Botek, E., and Péters de Bonhome, M.: The Mother’s Day Solar Storm of 11 May 2024 and Its Effect on Earth’s Radiation Belts, *Universe*, 10, 391, 2024.
- Randall, C., Harvey, V., Singleton, C., Bailey, S., Bernath, P., Codrescu, M., Nakajima, H., and Russell III, J.: Energetic particle precipitation effects on the Southern Hemisphere stratosphere in 1992–2005, *Journal of Geophysical Research: Atmospheres*, 112, 2007.
- 280 Rodger, C. J., Clilverd, M. A., Green, J. C., and Lam, M. M.: Use of POES SEM-2 observations to examine radiation belt dynamics and energetic electron precipitation into the atmosphere, *Journal of Geophysical Research: Space Physics*, 115, 2010.
- Rozanov, E., Calisto, M., Egorova, T., Peter, T., and Schmutz, W.: Influence of the precipitating energetic particles on atmospheric chemistry and climate, *Surveys in geophysics*, 33, 483–501, 2012.



- 285 Sætre, C., Stadsnes, J., Nesse, H., Aksnes, A., Petrinec, S., Barth, C., Baker, D., Vondrak, R., and Østgaard, N.: Energetic electron precipitation and the NO abundance in the upper atmosphere: A direct comparison during a geomagnetic storm, *Journal of Geophysical Research: Space Physics*, 109, 2004.
- Sátori, G., Williams, E., Price, C., Boldi, R., Koloskov, A., Yampolski, Y., Guha, A., and Barta, V.: Effects of energetic solar emissions on the Earth–ionosphere cavity of Schumann resonances, *Surveys in Geophysics*, 37, 757–789, 2016.
- 290 Seppälä, A., Matthes, K., Randall, C., and Mironova, I.: What is the solar influence on climate? Overview of activities during CAWSES-II. *Progress in Earth and Planetary Science*, 1, 24, DOI. ADS, 2014.
- Sinnhuber, M., Nieder, H., and Wieters, N.: Energetic particle precipitation and the chemistry of the mesosphere/lower thermosphere, *Surveys in Geophysics*, 33, 1281–1334, 2012.
- Smith, A. K. and Marsh, D. R.: Processes that account for the ozone maximum at the mesopause, *Journal of Geophysical Research: Atmospheres*, 110, 2005.
- 295 Smith, A. K., Espy, P. J., López-Puertas, M., and Tweedy, O. V.: Spatial and temporal structure of the tertiary ozone maximum in the polar winter mesosphere, *Journal of Geophysical Research: Atmospheres*, 123, 4373–4389, 2018.
- Verronen, P. and Lehmann, R.: Analysis and parameterisation of ionic reactions affecting middle atmospheric HO<sub>x</sub> and NO<sub>y</sub> during solar proton events, in: *Annales Geophysicae*, vol. 31, pp. 909–956, Copernicus Publications Göttingen, Germany, 2013.
- 300 Verronen, P., Rodger, C. J., Clilverd, M. A., and Wang, S.: First evidence of mesospheric hydroxyl response to electron precipitation from the radiation belts, *Journal of Geophysical Research: Atmospheres*, 116, 2011.
- Winant, A., Pierrard, V., and Botek, E.: Ozone decrease observed in the upper atmosphere following the May 11th 2024 Mother’s day solar storm: dataset., <https://doi.org/10.5281/ZENODO.14388032>, 2024.
- Xiong, S., Li, J., Wei, G., Lu, J., Tian, Y., Zhang, X., Fu, S., Sun, M., Li, Z., Zhang, H., et al.: The northern and southern hemispheric asymmetries of mesospheric ozone at high latitudes during the January 2012 solar proton events, *Space Weather*, 21, e2023SW003 435, 2023.
- 305